Enzymatic Transition States and Inhibitor Design from Principles of Classical and Quantum Chemistry

VERN L. SCHRAMM,* BENJAMIN A. HORENSTEIN, CAREY K. BAGDASSARIAN, STEVEN D. SCHWARTZ, PAUL J. BERTI, KATHLEEN A. RISING, JOHANNES SCHEURING, PAUL C. KLINE, DAVID W. PARKIN, AND DAVID J. MERKLER

Department of Biochemistry, The Albert Einstein College of Medicine of Yeshiva University, Bronx, New York 10461

Received February 29, 1996; accepted April 3, 1996

ABSTRACT

A procedure is described which leads to experimentally based models for the transition-state structures of enzyme-catalyzed reactions. Substrates for an enzymic reaction are synthesized with isotopically enriched atoms at every position in which bonding changes are anticipated at the enzyme-enforced transition state. Kinetic isotope effects are measured for each atomic substitution and corrected for diminution of the isotope effects from nonchemical steps of the enzymic mechanism. A truncated geometric model of the transition-state structure is fitted to the kinetic isotope effects using bond-energy bond-order vibrational analysis. Full molecularity is restored to the transition state while maintaining the geometry of the bonds which define the transition state. Electronic wave functions are calculated for the substrate and the transition-state molecules. The molecular electrostatic potential energies are defined for the van der Waal surfaces of substrate and transition state and displayed in numerical and color-coded constructs. The electronic differences between substrate and transition state reveal characteristics of the transition state which permits the extraordinary binding affinity of enzyme–transition state interactions. The information has been used to characterize several enzymatic transition states and to design powerfully inhibitory transition-state analogues. Enzymatic examples are provided for the reactions catalyzed by AMP deaminase, nucleoside hydrolase, purine nucleoside phosphorylase, and for several bacterial toxins. The results demonstrate that the combination of experimental, classical, and quantum chemistry approaches is

*To whom correspondence should be addressed.

International Journal of Quantum Chemistry: Quantum Biology Symposium 23, 1805–1813 (1996)

CCC 0360-8832 / 96 / 081805-09

capable of providing reliable transition-state structures and sufficient information to permit the design of transition-state inhibitors.

Introduction

Transition-state theory for enzymė-catalyzed reactions proposes that in the short lifetime of the transition state, the distorted substrate molecule binds tighter than in the initial enzyme–substrate complex by a factor equal to the rate enhancement imposed by the enzyme [1, 2]. With typical rate enhancements of 10^{10}–10^{15}, the dissociation constants for the transient transition-state complexes are commonly in the range of 10^{-13}–10^{-21} M, and thus represent a unique range of binding affinities among biological systems [3]. Transition-state inhibitor design attempts to capitalize on this binding energy by producing stable molecules which resemble an enzyme-bound transition state and thus bind tightly to form a stable, *inhibited* complex with the cognate enzyme. Exact duplicates of enzymatic transition states cannot be achieved because of the nonequilibrium bond lengths at the transition state. However, if only a small fraction of the binding energy is achieved, powerful inhibitors will result. Transition-state inhibitors also show unique specificity, in many cases showing specificity for a single isozyme among a family of enzymes which catalyze the same chemical reaction [4]. These observations have also demonstrated that transition-state structure is dependent on the nature of the enzymatic catalyst, in the same way that reactions in organic chemistry are often dependent on the nature of the solvent [5].

Accurate definition of the transition-state structures for enzyme-catalyzed reactions has remained elusive, but is an essential part in the design of transition-state inhibitors. The goal of the work presented here has been to establish a systematic experimental protocol which will provide enzymatic transition-state structures of sufficient accuracy to permit the direct characterization of enzymatic transition states. This information is of intrinsic interest in the investigation of the chemistry and mechanism of protein-based catalysts. In addition, the technique provides reliable information for the synthesis of transition-state analogues.

Experimental Methods

The procedure for establishing the geometry of an enzymatic transition-state structure is based on the Bigeleisen–Wolfsberg formulation [6, 7] which describes the perturbation of chemical equilibria by incorporation of isotopically enriched atoms. The theory is extended to a classical definition of the transition state [8] in which it is assumed that both the reactant and transition states are in thermal equilibrium with the environment and that the kinetic isotope effects are functions of the free-energy difference between reactant and transition states, adjusted for reaction-coordinate motion [9]. Specific isotopic substitutions at atomic positions whose bonding patterns are expected to be changed upon reaching the transition state can provide information for specific bond changes which occur on conversion of the reactant to the transition state [10, 11].

A family of labeled substrate molecules is synthesized with specific primary, secondary, and remote labels [12, 13]. Kinetic isotope effects are measured with each isotopically labeled substrate and any corrections applied which are necessary to interpret the kinetic isotope effects in terms of the chemistry which occurs at the enzymatic transition state. For accurate interpretation of the kinetic isotope effects into transition-state structure, bond breaking must be the highest energetic barrier on the reaction coordinate [14, 15]. The bond lengths and angles of a truncated atomic model of the transition state are analyzed by classical vibrational mode analysis [16, 17] in which the reactant structure is compared with systematically varied transition-state structures until the experimental kinetic isotope effects are reproduced by the transition-state model, using logical principles of chemical bonding [18–21]. The bonds established from the kinetic isotope effects are fixed and the structure restored to full molecularity, using molecular energetic minimization methods imple-

mented in MOPAC and/or Gaussian routines [22, 23] to provide structural optimization while maintaining the distorted bonds of the transition state which are established from the kinetic isotope effects.

The substrate is analyzed in a similar manner, starting with the X-ray crystal or nuclear magnetic resonance (NMR) structure where available, and followed by determination of the energetic minimum of the full molecule, including hydrogens, using Gaussian energy minimization. Optimized bond geometries provide information to permit solution of an electronic wave function for both the substrate and the transition state [24, 25]. The molecular electrostatic potential at the van der Waal surface is extracted from the wave function and provides electrostatic models which can be compared for the features which are unique to the transition state. These are candidates for the tight-binding interactions of the enzyme–transition state complex. Binding features include hydrogen bond donor and acceptor sites, ionic bonding sites, and hydrophobic sites. All such sites are identified in the molecular electrostatic potential surface of the substrate and transition state by color-coding the numerical values of the electrostatic potential using AVS Chem Viewer [26, 27]. Electrostatic recognition sites, which change position and/or bonding character on conversion from reactant molecule to transition state molecule, are sites to be incorporated into the proposed transition-state inhibitor [3].

Results

The ability to predict enzymatic transition states can be tested by comparing experimentally determined transition states with natural products which are known to be transition state inhibitors. In addition, the procedure for transition-state analysis based on kinetic isotope effects provides geometric and electronic models of enzymatic transition states which have been used as practical blueprints for the construction of transition-state inhibitors [27–29]. The procedure has been applied to several test case enzymes.

AMP DEAMINASE

AMP deaminase from yeast catalyzes the hydrolytic deamination of adenosine 5′-monophosphate (AMP) to inosine 5′-monophosphate (IMP) and ammonia (Fig. 1). The enzyme has been proposed to regulate the energy metabolism of the organism by controlling the level of AMP in the cell [30]. The X-ray crystal structure of a closely related enzyme, adenosine deaminase, established that the reacting water molecule is bound to an enzymatic zinc ion to form a reactive hydroxyl ion nucleophile [31].

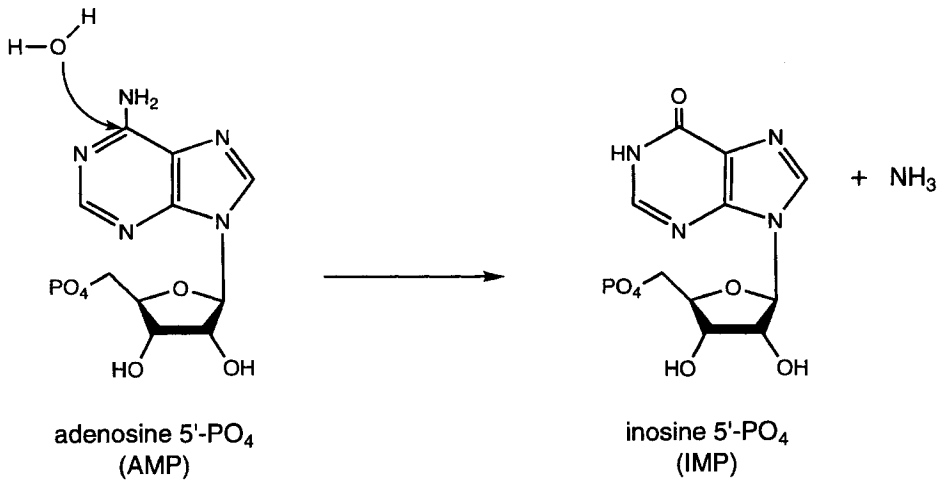

FIGURE 1. Reaction catalyzed by AMP deaminase. At the transition state the attacking H_2O has a bond order of 0.8 to the carbon and the $—NH_2$ remains fully bonded. This configuration is shown in Figure 2(b).

AMP deaminase also contains zinc, and all amino acids in contact with the zinc and the purine base of the substrate for adenosine deaminase are strictly conserved in AMP deaminase, indicating that both enzymes use zinc-activated hydroxide as the attacking water nucleophile [32].

The purpose of this study was to establish the nature of the enzyme-stabilized transition state structure and to compare it with a natural product transition-state inhibitor. The inhibitor coformycin 5′-phosphate binds 5×10^7 times more tightly than substrate, making it one of the most powerful enzymatic inhibitors. The kinetic isotope effects for the AMP deaminase reaction were measured with [6-^{14}C]AMP and natural abundance [6-^{15}N]AMP substrates and matched to a reaction mechanism in which attack of the zinc-bound water nucleophile is the highest barrier on the reaction coordinate [33]. At the transition state, the bond order to the attacking water nucleophile is 0.8, while the departing ammonia group remains as an NH_2, and has not yet accepted the proton required to form the NH_3 group prior to its departure. The addition of nearly a full bond order by the attacking hydroxyl rehybridized the carbon at the reaction center from sp^2 to sp^3, and caused loss of the conjugation of the ring and enzymatic protonation of N1 by a specific glutamic acid in the catalytic site (see Fig. 1).

These features of the transition state were maintained while full molecularity was added to the purine ring using MOPAC [22]. The electronic wave functions were then calculated for the substrate, transition state, and the transition-state inhibitor using Gaussian 92. The molecular electrostatic potential surfaces for substrate, transition state, and transition state inhibitor were extracted at the van der Waal surface, defined as $0.002e/a_0^3$ [34]. The structures of the 9-methyl derivatives of substrate, transition state, and transition-state inhibitor are shown in Figure 2(A)–(C) respectively, and the molecular electrostatic potential surfaces are displayed in Figure 3(A)–(C) by color coding the electrostatic potentials at the van der Waal surfaces. The results demonstrate that the substrate and transition state [Fig. 3(A) and 3(B)] differ in both shape and in their molecular electrostatic potentials [35]. The remarkable geometric and electrostatic similarity of the transition state and transition-state inhibitor [Fig. 3(B) and 3(C)] provides evidence that the electrostatic potential is a major determinant in permitting matches between the transition state and transition-state inhibitors.

IU-NUCLEOSIDE HYDROLASE

Protozoan parasites contain several enzymes which catalyze hydrolysis of the N9-C1′ bond of nucleosides according to the reaction:

$$\text{Nucleoside} + H_2O \rightarrow \text{base} + \text{ribose}$$

and which function in the salvage of exogenous purines, since the organisms have lost the ability for de novo purine synthesis. Mammals have retained de novo purine biosynthesis and do not contain the nucleoside hydrolases. Thus, the nucleoside hydrolases are inhibitory targets for protozoan-specific antibiotic design [36]. Transition-state theory for enzyme-catalyzed reactions proposes that stable compounds which mimic enzymatic transition states will be powerful inhibitors. The goal of this study was to establish the transition-state structure for a nucleoside hydrolase and to incorporate features of the transition state into inhibitors for the nonspecific inosine-uridine nucleoside hydrolase (IU-nucleoside hydrolase) isolated from the trypanosome *Crithidia fasciculata*.

Inosine molecules with the appropriate isotopic labels were synthesized and used to measure a family of kinetic isotope effects which were also compared to isotope effects for acid-catalyzed chemical solvolysis of similar molecules [18, 20] (Table I). Bond-energy bond-order vibrational analysis of the kinetic isotope effects gave a transition-state structure with nearly complete loss of the ribose-purine C1′-N9 bond, low bond order to the attacking water nucleophile, substantial rehybridization of the bonding ribose carbon C1′ from sp^3 to sp^2, development of partial positive charge in the ribosyl oxocarbenium, and enzymatic protonation of the leaving group at N7. Full molecular structure was added, the bonds defined by kinetic isotope effects were fixed, and the bond lengths and angles to the remainder of the atoms optimized using the MOPAC routine [20]. Determination of the electron wave function, and display of the molecular electrostatic potential surfaces as described above resulted in the substrate and transition-state structures shown in Figures 2(D) and (E) and 3(D) and (E) [26].

Synthesis of a family of transition-state analogues based on the geometric and electronic features of the transition state resulted in a group of inhibitors which bind up to 2×10^5 times tighter

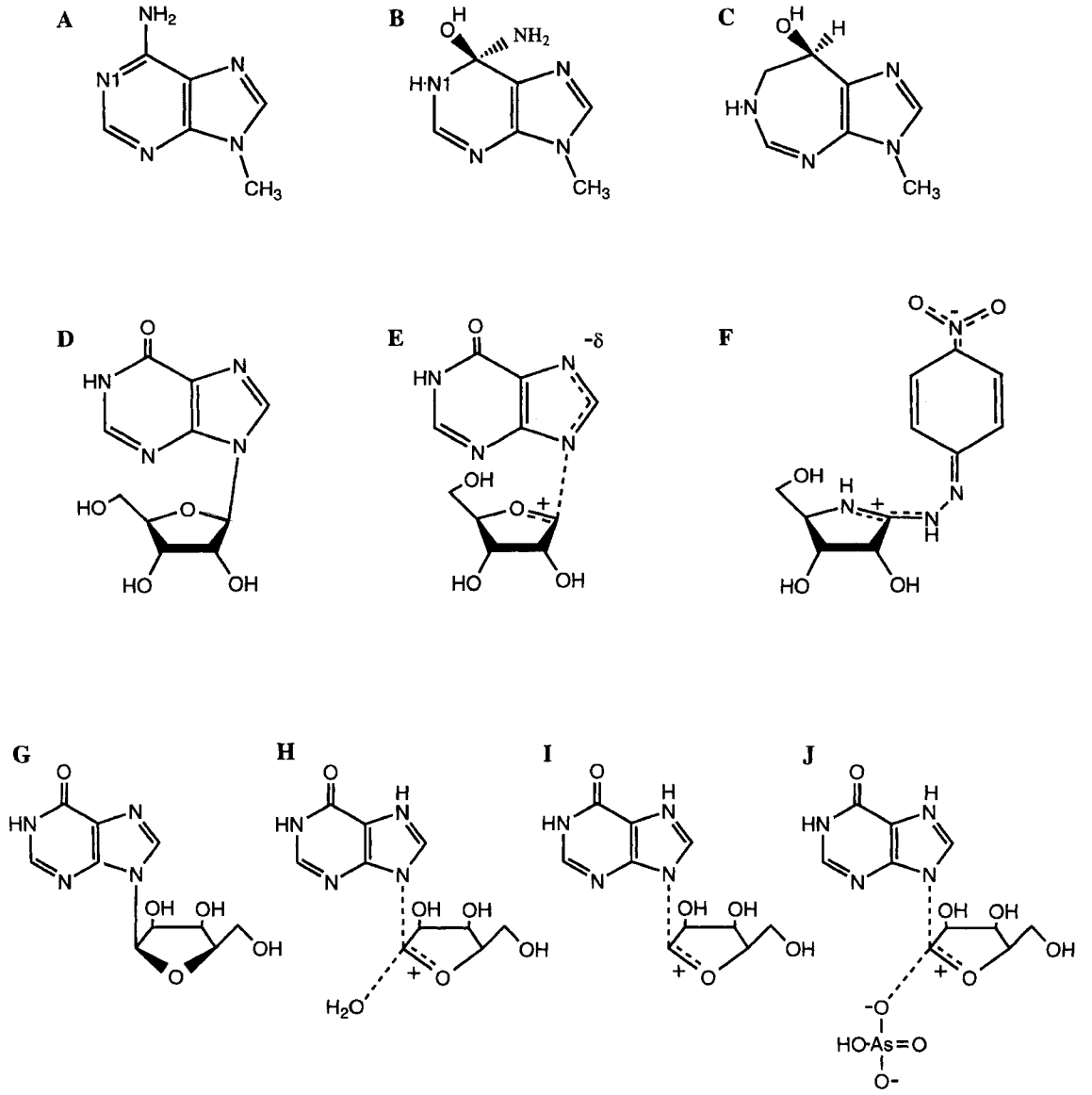

FIGURE 2. Chemical models used for electrostatic potential surface analysis of the AMP deaminase reaction are truncated by replacing the ribose 5-phosphate with a methyl group, since the ribose 5-phosphate does not participate in the reaction coordinate. The substrate and transition state are A and B, respectively. The transition state bond lengths and angles are compared to those of the substrate in [35]. The methyl derivative of coformycin 5′-phosphate (C) is the transition-state inhibitor of AMP deaminase. The substrate inosine, transition state, and transition-state inhibitor for the IU-nucleoside hydrolase reaction are shown in (D), (E), and (F), respectively. The N7 protonation and the enzyme-activated water nucleophile which are part of the transition-state ensemble are not shown in (E). Both kinetic isotope effects and X-ray crystallographic studies indicate the rotation of the 5′-OH in the transition state. The tautomeric form of the bound transition state inhibitor, nitrophenylriboamidrazone (F), has been established by resonance Raman studies [39]. The substrate and transition states for the purine nucleoside phosphorylase are shown in (G) –(I). The substrate inosine (G) is shown in the anti-ribosyl configuration as are the three transition state structures (H) –(J). The transition state for the hydrolytic reaction is shown with (H) and without (I) the attacking water nucleophile. The transition-state structure for arsenolysis is shown in (J). These results are from [37], which provides detailed information on bond lengths and angles in substrate and transition states.

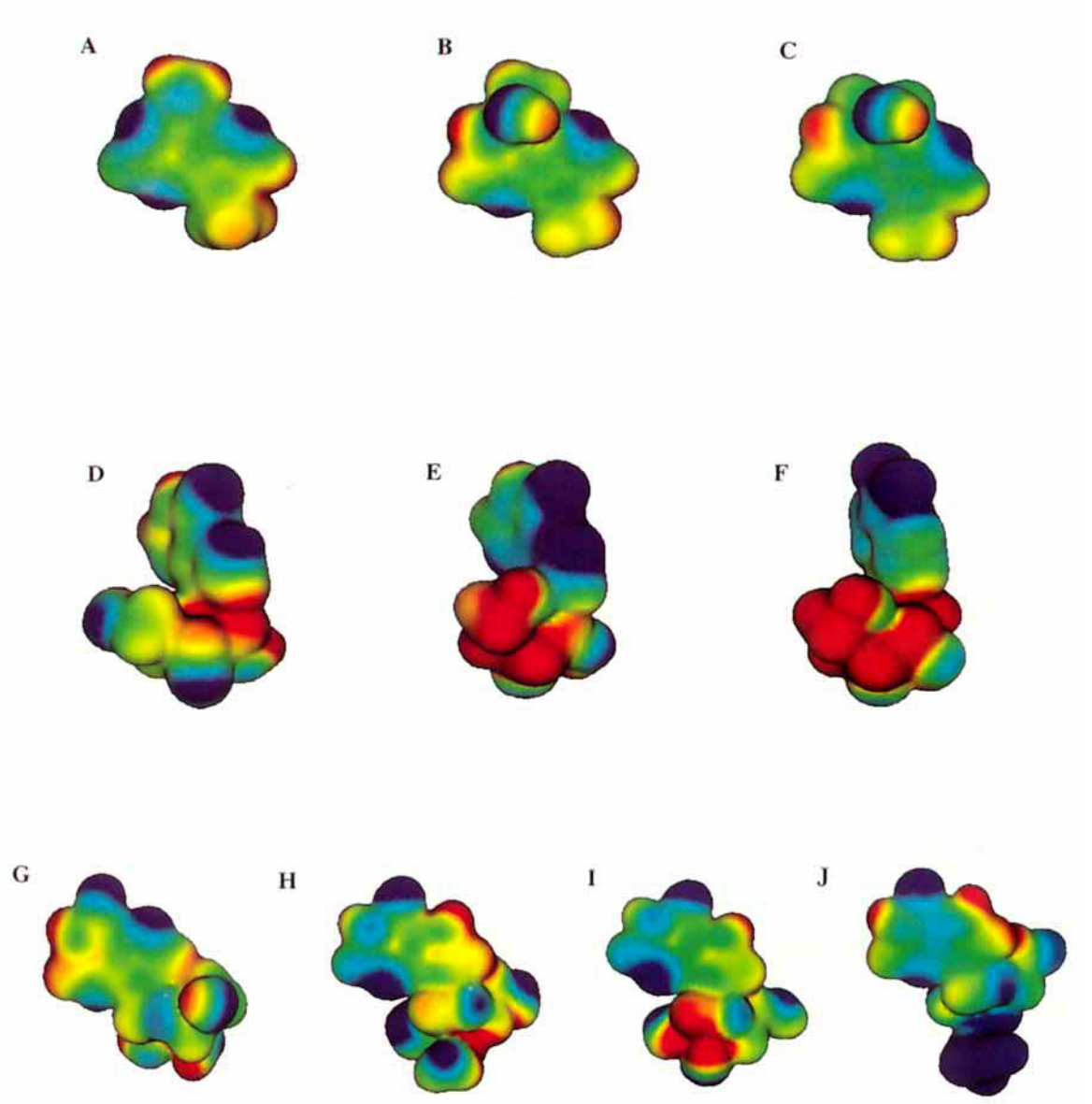

FIGURE 3. Molecular electrostatic potential surfaces which correspond to the structures (A) –(J) in Figure 2. Blue indicates areas of partial negative charge and red indicates partial positive charge (electron rich and electron deficient, respectively). The substrate, transition state, and transition-state inhibitor for AMP deaminase are indicated in (A) –(C). Note the similarity of (B) and (C) and that both differ substantially from (A). The substrate, inosine, transition state, and transition-state inhibitor for IU-nucleoside hydrolase are shown in (D) –(F), respectively. Note the similarity of (E) and (F) and that both differ substantially from (D). The red electron deficient area in (E) is due to the formation of the oxocarbenium ion at the transition state. In (F), the red electron deficient area is due to the tautomeric configuration of the *N*-ribosyl-amidrazone group. On the enzyme, both of these sites interact with an enzyme-bound water nucleophile to provide partial neutralization of this charge. The substrate inosine (G) and three transition state structures [(H) –(J)] are shown for purine nucleoside phosphorylase. In (H), the transition state includes the attacking water nucleophile 3.0 Å from the C1′ of ribose. Note the charge neutralizing effect relative to I, the same transition state without the influence of the attacking water. The transition state for the arsenolysis reaction (J) includes the attacking arsenate anion which completely neutralizes the positive charge of the oxocarbenium transition state.

TABLE I

Kinetic isotope effects for the chemical and enzymatic hydrolysis and arsenolysis of nucleosides.[a]

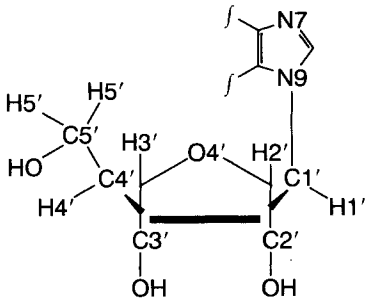

Kinetic Isotope Effect	Acid Catalyzed[b]	IU-Nucleoside Hydrolase[c]	Purine Nucleoside Phosphorylase[d]
^{15}N9	3.0 ± 0.2	2.6 ± 0.4	1.0 ± 0.5
^{14}C1′	4.4 ± 0.3	4.4 ± 0.4	2.6 ± 0.6
^{3}H1′	21.6 ± 0.4	15.0 ± 0.6	14.1 ± 0.4
^{3}H2′	11.3 ± 0.2	16.1 ± 0.3	15.2 ± 0.3
^{3}H4′	—	−0.8 ± 0.3	0.8 ± 0.4
^{3}H5′	0.6 ± 0.2	5.1 ± 0.3	3.3 ± 0.5

[a]The isotope effects are presented as (kinetic isotope effect −1.000) (100). Thus, these are percentage isotope effects. The determination of these kinetic isotope effects are described in references [18],[b] [20],[c] and [37],[d] respectively. The attacking nucleophiles are H_2O for the acid and nucleoside hydrolase reactions and is arsenate for purine nucleoside phosphorylase. The purine ring is truncated since inosine, adenosine, and AMP were used in these studies.

than substrate [27, 29]. One of these inhibitors, *p*-nitrophenyl-riboamidrazone, a 2 *nM* inhibitor, is shown in Figures 2(F) and 3(F). The strong similarity between both the geometric and electrostatic features of the transition state and transition-state inhibitor demonstrates the significance of obtaining transition-state information and using that information to match the electrostatic features of the transition state to achieve transition-state inhibitors [3].

PURINE NUCLEOSIDE PHOSPHORYLASE

Purine nucleoside phosphorylase catalyzes the phosphorolysis of purine nucleosides:

$$\text{Purine nucleosides} + PO_4 \rightarrow \text{purine base} + \text{ribose 1-phosphate}$$

but can also utilize arsenate in the place of phosphate or can hydrolyze the purine nucleosides very slowly if phosphate or arsenate are missing. This difference in the nature of the nucleophilic group provided the opportunity to determine the transition-state structure for an enzyme catalyzed reaction in which the attacking nucleophile varies in charge. The kinetic isotope effects were measured and are compared to those obtained with IU-nucleoside hydrolase in Table I. The transition-state structure was obtained by bond-energy bond-order vibrational analysis, MOPAC optimization, Gaussian determination of the electron wave function, extraction of the molecular electrostatic potential surface, and display of the van der Waal electrostatic potential [37].

The structures shown in Figures 2(G)–(J) and 3(G)–(J) represent the substrate inosine (G), the transition state with an attacking water nucleophile (H), the transition-state inosine with the attacking nucleophile removed to demonstrate the positive charge on the oxocarbenium (I), and the transition state with the attacking arsenate anion (J). The presence of the arsenate increases the reaction rate approximately four orders of magnitude relative to the hydrolytic reaction whose transition state is shown in Figures 2 and 3(H). The dianionic arsenate neutralizes the partial positive charge developing on the oxocarbenium, thus assisting formation of the transition state. The change in electrostatic potential which accompanies the conversions of substrates to transition states is substantial, and underscores the conclusion that the distinct features of the transition state are responsible for the differential binding of substrates and transition-state analogues illustrated above.

ADP-RIBOSYLATING TOXINS

Hydrolytic and transfer reactions of N–C ribosidic bonds forms an important segment of biological reactions. One example now under investigation is the action of bacterial ADP-ribosylating toxins [38]. Cholera, diphtheria, and pertussis toxins have the common reaction:

$$NAD^+ + \text{GTP-binding protein} \xrightarrow{\text{toxin}} \text{ADP-ribosylated GTP binding protein} + \text{nicotinamide}$$

When the acceptor GTP-binding proteins are absent, all of these toxins catalyze hydrolysis of NAD^+. Transition-state analysis of these reactions

requires synthesis of NAD^+ with the specific incorporation of isotopically enriched atoms. This has been accomplished using an enzyme-based synthetic chemistry [13]. Isotope effects for the toxins suggest that all three of the toxins enforce dissociative, S_N1 reaction mechanism when hydrolysis of NAD^+ occurs.

Discussion and Conclusions

The combination of experimental kinetic isotope effects, classical bond vibrational analysis, molecular mechanics, construction of electronic wave functions and the molecular electrostatic potential surfaces of substrates, transition states, and transition-state inhibitors provides reliable models which can be used to understand enzyme-stabilized transition states and to design transition-state inhibitors. The studies provide novel insights into the molecular distortions which constitute enzymatic transition states. The experimental data are adequate for the prediction of compounds which will act as transition state inhibitors for the target enzymes.

ACKNOWLEDGMENTS

This research program has been developed with research funds supplied by the National Institutes of Health, the American Cancer Society, and the G. Harold and Leila Y. Mathers Charitable Foundation.

References

1. L. Pauling, Am. Sci. **36**, 50 (1948).
2. R. Wolfenden, Ann. Rev. Biophys. Bioeng. **5**, 271 (1976).
3. V. L. Schramm, B. A. Horenstein, and P. C. Kline, J. Biol. Chem. **269**, 18259 (1994).
4. B. Estupiñán and V. L. Schramm, J. Biol. Chem. **269**, 23068 (1994).
5. C. Reichardt, in *Solvents and Solvent Effects in Organic Chemistry*, 2nd ed. (VCH Publishers, New York, 1985).
6. J. Bigeleisen and M. G. Mayer, J. Chem. Phys. **15**, 261 (1947).
7. J. Bigeleisen and M. Wolfsberg, Adv. Chem. Phys. **1**, 15 (1958).
8. S. Glasstone, K. J. Laidler, and H. K. Eyring, *The Theory of Rate Processes* (McGraw-Hill, New York, 1941).
9. W. P. Huskey, in *Enzyme Mechanism from Isotope Effects*, Cook, P. F., Ed., (CRC Press, Boca Raton, FL, 1991), pp. 37–72.
10. L. B. Sims, G. W. Burton, and D. E. Lewis, BEBOVIB-IV, Quantum Chemistry Program Exchange, No. 337, Indiana University, Bloomington, IN, 1977.
11. G. W. Burton, L. B. Sims, J. C. Wilson, and A. Fry, J. Am. Chem. Soc. **99**, 3371 (1977).
12. D. W. Parkin, H. B. Leung, and V. L. Schramm, J. Biol. Chem. **259**, 9411 (1984).
13. K. A. Rising and V. L. Schramm, J. Am. Chem. Soc. **116**, 6531 (1994).
14. D. B. Northrop, Ann. Rev. Biochem. **50**, 103 (1981).
15. W. W. Cleland, Methods Enzymol. **87**, 625 (1982).
16. L. B. Sims and D. E. Lewis, in *Isotopes in Organic Chemistry*, Vol. 6, E. Buncel and C. C. Lee, Eds. (Elsevier, New York, 1984), pp. 161–259.
17. J. Rodgers, D. A. Femec, and R. L. Schowen, J. Am. Chem. Soc. **104**, 3263 (1982).
18. F. Mentch, D. W. Parkin, and V. L. Schramm, Biochemistry **26**, 921 (1987).
19. G. D. Markham, D. W. Parkin, F. Mentch, and V. L. Schramm, J. Biol. Chem. **262**, 5609 (1987).
20. B. A. Horenstein, D. W. Parkin, B. Estupinan, and V. L. Schramm, Biochemistry **30**, 10788 (1991).
21. P. C. Kline and V. L. Schramm, Biochemistry **34**, 1153 (1995).
22. K. M. Merz, Jr., and B. H. Besler, Quantum Chemistry Program Exchange, No. 589, Indiana University, Bloomington, IN, 1990.
23. M. J. Frisch, G. W. Trucks, M. Hend-Gordon, P. M. W. Gill, M. W. Wong, J. B. Foresman, B. G. Johnson, H. B. Schlegel, M. A. Robb, E. S. Replogle, R. Gomperts, J. L. Andres, K. Raghavachari, J. S. Binkley, C. Gonzalez, R. L. Martin, D. J. Fox, D. J. DeFrees, J. Baker, J. J. P. Stewart, and J. A. Pople, Gaussian 92 User's Guide, Gaussian Inc., Pittsburgh, 1992.
24. P. Politzer and G. Truhlar, Eds., *Chemical Applications of Atomic and Molecular Electrostatic Potentials* (Plenum Press, New York, 1981).
25. S. Srebrenik, H. Weinstein, and R. Pauncz, Chem. Phys. Lett. **20**, 419 (1973).
26. B. A. Horenstein and V. L. Schramm, Biochemistry **32**, 7089 (1993).
27. B. A. Horenstein and V. L. Schramm, Biochemistry **32**, 9917 (1993).
28. B. A. Horenstein, R. F. Zabinski, and V. L. Schramm, Tet. Lett. **34**, 7213 (1993).
29. M. Boutellier, B. A. Horenstein, A. Semenyaka, V. L. Schramm, and B. Ganem, Biochemistry **33**, 3994 (1994).
30. D. J. Merkler, A. S. Wali, J. Taylor, and V. L. Schramm, J. Biol. Chem. **264**, 21422 (1989).
31. D. K. Wilson, F. B. Rudolph, and F. A. Quiocho, Science **252**, 1278 (1991).
32. D. J. Merkler and V. L. Schramm, Biochemistry **32**, 5792 (1993).
33. D. J. Merkler, P. C. Kline, P. Weiss, and V. L. Schramm, Biochemistry **32**, 12993 (1993).
34. P. Sjoberg and P. Politzer, J. Phys. Chem. **94**, 3959 (1990).
35. P. C. Kline and V. L. Schramm, Biochemistry **34**, 1153 (1994).

36. D. W. Parkin, B. A. Horenstein, D. R. Abdulah, B. Estupinan, and V. L. Schramm, J. Biol. Chem. **266**, 20658 (1991).
37. P. C. Kline and V. L. Schramm, Biochemistry **32**, 13212 (1993).
38. K. Aktories, Ed. *Current Topics in Microbiology and Immunology. ADP-Ribosylating Toxins* (Springer-Verlag, Berlin, 1992).
39. H. Deng, A. W.-Y. Chan, C. K. Bagdassarian, B. Estupiñán, B. Ganem, R. H. Callender, and V. L. Schramm, Biochemistry **35**, 6037 (1996).